

Lensless Compound-Eye Vision with Plasmonic Ommatidia

L. C. Kogos, Y. Li, J. Liu, Y. Li, L. Tian, and R. Paiella*

Department of Electrical and Computer Engineering and Photonics Center, Boston University, 8 St. Mary's St., Boston, MA 02215

*Corresponding author: rpaiella@bu.edu

Abstract: We report the design, fabrication, and characterization of geometrically-tunable angle-sensitive photodetectors based on plasmonic metasurfaces for the development of flat lensless compound-eye cameras with ultrawide ($\pm 75^\circ$) fields of view. © 2020 The Authors

OCIS codes: (230.0230) Optical devices; (240.6680) Surface plasmons; (110.2970) Image detection systems.

1. Introduction

Inspired by the vision system of small animals such as insects and crustaceans, artificial compound-eye cameras are uniquely suited to applications requiring large fields of view, extreme size miniaturization, and high sensitivity to motion [1]. Compound eyes in nature typically consist of a curved array of individual imaging elements (ommatidia) pointing along different directions, each collecting a single point of information about the scene being imaged. Unfortunately, however, the development of artificial cameras that directly mimick the compound eyes of common arthropods is severely complicated by their curved geometry, which is not directly compatible with standard microelectronic circuits and therefore requires the introduction of complex fabrication and packaging processes [2]. Here, we describe a compound-eye camera technology based on a fundamentally different approach that can provide wide-angles field of view (over $\pm 75^\circ$) on a flat substrate without any lenses [3]. Its key innovation is the integration of each pixel of a standard image-sensor array with a specially designed plasmonic metasurface that only allows for the detection of light incident along a small, geometrically tunable distribution of angles, whereas light incident along all other directions is reflected. Computational imaging techniques are then employed to enable image reconstruction from the combined signals of the individual sensors.

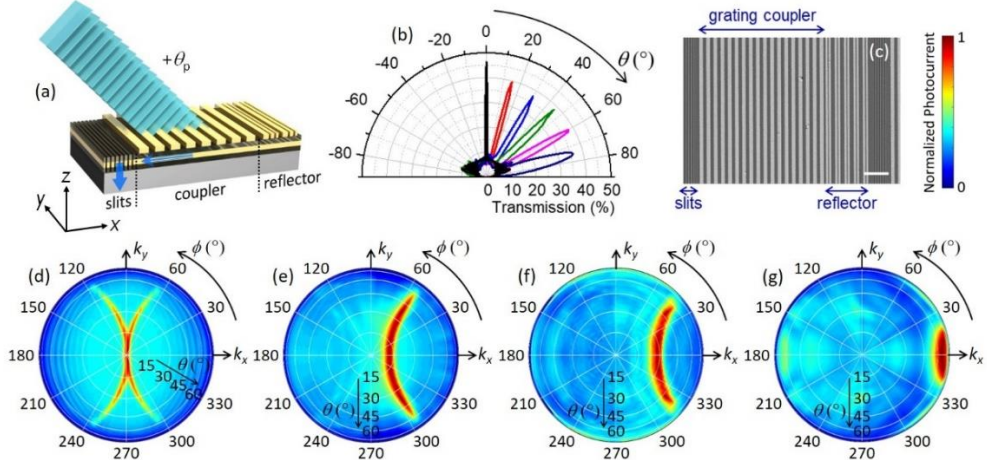


Fig. 1. (a) Schematic illustration of the device geometry and operation principle. (b) Calculated optical transmission coefficient at $\lambda_0 = 1550$ nm through six different metasurfaces for p polarized light versus angle of incidence θ on the x - z plane. (c) Optical image of a representative experimental sample. The scale bar is 4 μ m. (d)-(g) Measured angular dependence of the photocurrent of four different samples based on the design set of (b). The devices are illuminated with laser light at 1550 nm and each map is summed over two orthogonal polarizations.

2. Results and discussion

The principle of operation of our angle-sensitive devices is illustrated in Fig. 1. The photodetector active material (a Ge photoconductor) is coated with a metal film stacked with an array of rectangular metallic nanoparticles (NPs). The metal film is sufficiently thick (~ 100 nm) to block any externally incident light from propagating directly into the underlying active layer. Therefore, photodetection in this geometry can only take place through an indirect process [Fig. 1(a)] where light incident at the desired detection angle $+θ_p$ is first diffracted by the NPs (in the periodic “grating coupler” section of the array) into surface plasmon polaritons (SPPs) on the top surface of the metal film. A small number of suitably positioned subwavelength slits in the metal film are then used to scatter these SPPs into radiation propagating predominantly into the absorbing active layer, and as a result a photocurrent signal is produced. Light incident along any other direction is instead either immediately reflected by the metal film, or diffracted into SPPs

propagating towards the “grating reflector” section of the NP array, which comprises a phase-gradient metasurface designed to scatter the incoming SPPs back into the air above.

In the present work, we have developed a set of directional photodetectors based on this approach with different polar angles of peak detection ranging from 0° to 75° in steps of 15° . The metasurfaces were designed via rigorous electromagnetic simulations for operation at a target wavelength $\lambda_0 = 1550$ nm [Fig. 1(b)]. Experimental samples [Fig. 1(c)] were developed using standard fabrication processes including electron-beam lithography and thermal evaporation. The color maps of Figs. 1(d)-(g) show the photocurrent signals measured with four different devices as a function of polar θ and azimuthal ϕ illumination angles. In each map, the incident directions of high photocurrent form a rather narrow region within the full hemisphere, with a distinctive C shape determined by first-order diffraction of the incoming light into different SPP modes. The experimental device characteristics, including angular resolution, peak responsivity, and peak-to-background ratio, are in good agreement with numerical simulations [3].

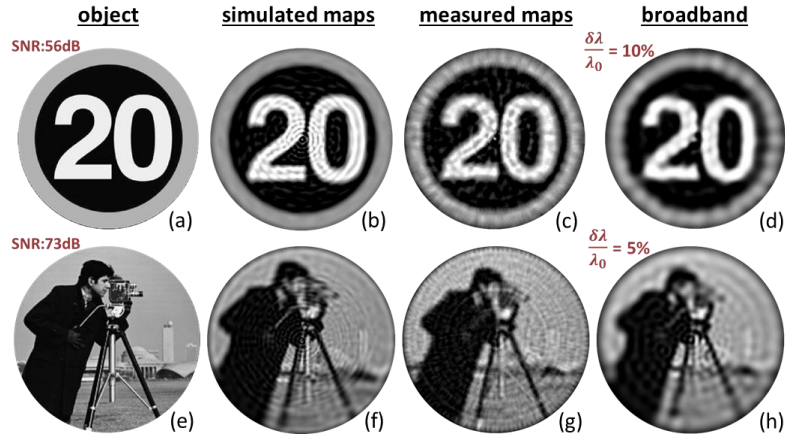


Fig. 2. Image reconstruction results. (a)-(d) Representative object (a) and corresponding images reconstructed for SNR = 56 dB (b)-(d). (e)-(h) Example of a more complex object (e) and corresponding images reconstructed for SNR = 73 dB (f)-(h). The images of (b) and (f) are based on the simulated responsivity patterns with a 6240-pixel array at $\lambda_0 = 1550$ nm. The images of (c) and (g) are based on the experimental responsivity patterns with a 5280-pixel array at $\lambda_0 = 1550$ nm. The images of (d) and (h) are based on the simulated patterns with a 6240-pixel array under broadband illumination with bandwidth $\delta\lambda/\lambda_0 = 10\%$ (d) and 5% (h).

To evaluate the imaging capabilities of these devices, we have conducted a series of numerical simulations based on computational imaging techniques [3]. In these simulations, we consider an array of $\sim 6,000$ pixels, each coated with a metasurface providing directional photodetection peaked at a different combination of polar and azimuthal angles (θ_p and ϕ_p , respectively). Each pixel is described by its angular response map, i.e., photocurrent versus illumination angles. In our design and experimental work reviewed above, we have calculated and measured the angular response maps of a small number (six) of different devices with different values of θ_p for $\phi_p = 0^\circ$ [examples are shown in Figs. 1(d)-(g)]. The map of every other pixel in the camera is then constructed with a linear interpolation based on these six original maps. White Gaussian noise is also included in the simulations, for different values of signal-to-noise ratio (SNR) achievable with current CMOS image-sensor technology.

Examples of reconstructed images are shown in Fig. 2 for two objects of different complexity [panels (a) and (e)] across a field of view of about $\pm 75^\circ$. For each object, we present images reconstructed based on both simulated [(b), (f)] and measured [(c), (g)] angular response maps. Additionally, we have also extended our computational imaging framework to enable image reconstruction under polychromatic illumination with finite optical bandwidth $\delta\lambda$ [(d), (h)]. Both objects are well reproduced in all images, despite some loss of resolution which is intrinsic to the compound-eye vision modality [1]. These devices are therefore promising for the development of a new camera technology featuring the unique attributes of the compound eye, including ultrawide field of view (nearly full hemispherical), small size, and high temporal bandwidth resulting from infinite depth of field. These properties are ideally suited for applications such as endoscopy, swallowable or implantable cameras, and autonomous navigation.

This work was supported by NSF under Grant ECCS-1711156.

3. References

- [1] M. F. Land and D. E. Nilsson, *Animal Eyes* (Oxford University Press, Oxford, 2002).
- [2] Y. M. Song, Y. Xie, V. Malyarchuk, J. Xiao, I. Jung, K.-J. Choi, Z. Liu, H. Park, C. Lu, R.-H. Kim, R. Li, K. B. Crozier, Y. Huang, and J. A. Rogers, “Digital cameras with designs inspired by the arthropod eye,” *Nature* **497**, 95-99 (2013).
- [3] L. Kogos, Y. Li, J. Liu, Y. Li, L. Tian, and R. Paiella, “Plasmonic ommatidia for lensless compound-eye vision,” *Nat. Commun.* **11**, 1637 (2020).